Effect of ^{176}Lu Background on Singles Transmission for LSO-based PET Cameras

J.S. Huber†, W.W. Moses†, W.F. Jones‡, and C.C. Watson‡

†Lawrence Berkeley National Laboratory, University of California, Berkeley, CA 94720

‡CTI PET Systems, Inc., Knoxville, TN 37932

Abstract

We explore how radioactive background from naturally occurring ^{176}Lu affects single photon transmission imaging for Lutetium Orthosilicate (LSO) scintillator-based PET cameras by estimating the transmission noise equivalent count rate (NECR) including this background. Assuming a typical PET camera geometry (80 cm detector ring diameter), we use a combination of measurement and analytic computation to estimate the counting rates due to transmission, scatter, and background events as a function of singles transmission source strength. We then compute a noise equivalent count rate (NECR) for singles transmission. We find that the presence of the natural background radiation reduces the NECR by 60% or higher for source strengths less than 10 mCi, and that a 25% reduction of the NECR can occur even with a source strength of 40 mCi.

Introduction

Since its discovery approximately ten years ago [1], LSO (cerium activated lutetium oxyorthosilicate or Lu_2SiO_5:Ce) has shown great promise as a PET scintillator because of its unique combination of short attenuation length, high light output, and short decay time.

This work was supported in part by the U.S. Department of Energy under contract No. DE-AC03-76SF00098, and in part by the Public Health Service Grants No.s PO1-HL25840 and RO1-CA67911.

The first PET scanner to utilize LSO is for imaging small animals [2, 3], but a large variety of PET detector modules utilizing LSO have since been completed or are under development [4-12]. Another recent trend in PET instrumentation has been a renewed interest in "singles transmission" for PET, where a ^{137}Cs source that emits single gamma rays (rather than a ^{68}Ge source that emits positrons) is used to obtain an attenuation map by performing what is essentially an x-ray CT scan. Attenuation correction in PET using a single photon transmission measurement has a higher count rate capability at the cost of additional scatter contamination, because conventional PET transmission using a positron source is limited by near-side detector dead time [13-17]**.** These two trends have converged, resulting in a LSO-based PET camera that employs a singles transmission source [9]**.**

Despite its many advantages as a scintillator for PET, the lutetium in LSO contains approximately 2.6% ^{176}Lu, a naturally occurring radioisotope with a $4x10^{10}$ year half life. This leads to a background count rate of approximately 240 cps per cc of scintillator material over the full spectrum [1]**.** This generates a negligible coincident background event rate, and so has been ignored in PET cameras. The purpose of this paper is to explore the effect of this background on the singles transmission measurement, which does not have the background rejection afforded by coincidence timing.

Methods

In order to quantitatively evaluate the affect of ^{176}Lu background, we use the transmission noise equivalent count (NECR) metric [18, 19] that has been modified to include the ^{176}Lu background contribution, as the statistical error from the ^{176}Lu radiation lowers the NECR even after the average background rate is subtracted. The underlying assumption is that the quality of the transmission measurement depends only on the statistical accuracy of that measurement, and so two techniques that have the same

NECR will produce equally accurate measurements when they accumulate data for the same length of time. We compute the NECR for singles transmission as:

$$\text{NECR} = Tr^2 L/(Tr+S+LSO) \quad (1)$$

where *Tr*, *S* and *LSO* are the transmission, scatter and ^{176}Lu background rates respectively and *L* is the system livetime. No term for randoms is included, as it is not relevant for singles transmission. The transmission, scatter, and background event rates all depend linearly on the front surface area of the detector module, so the relative fractions of these three rates are independent of module front surface area. We therefore quote rates for a single detector module assuming a "typical" whole body cylindrical PET camera with 80 cm diameter detector ring, a ^{137}Cs point source that orbits at a distance of 70 cm from the "far" detector, and each detector module having a 51x51 mm^2 front surface. Changing the assumption to include more modules, different size modules, or multiple source geometries will not affect the conclusions, since all three rates (transmission, scatter, and background) will scale by the same factor and so their ratios will be unchanged. Different assumptions for the ring diameter and source orbit diameter will change results somewhat, as the ratio of background events to transmission events depends on these distances. We assume pre-injection transmission acquisition, so we have not included emission background contributions that can be significant for post-injection transmission acquisition.

Estimates of the flux of unattenuated transmission events on the detector module are based on geometrical factors and are multiplied by a patient attenuation factor to predict the attenuated flux. We consider two different values for the attenuation factor: the mean factor (*i.e.,* the mean of all chords having non-zero attenuation) and the maximum factor (*i.e.,* the chord with the highest attenuation, typically from chords that pass through both shoulders). We have determined these factors from measured attenuation values in whole

body chest and thorax studies, and we find a mean attenuation factor of 15 and a maximum attenuation factor of 74. The transmission event rate further takes into account the branching ratio of ^{137}Cs into a single gamma (85%) and the probability of absorption and detection in the detector modules, including a 14% loss due to the saw cuts in the module. Two detector module assumptions are explored: a "low" and "high" performance version, with the relevant assumptions for each shown in Table 1. Others have shown the transmission scatter fraction to be 21% of the mean transmission rate for a water-filled 20 cm diameter cylindrical phantom for uncollimated and 6% for collimated transmission data [20]**.** We use similar factors, also shown in Table 1, to estimate scatter rates.

	"Low" Performance	"High" Performance
Dead Time (paralyzing)	1000 ns	500 ns
Detector Thickness	15 mm	30 mm
Scatter Fraction (collimated)	6%	6%
Scatter Fraction (uncollimated)	25%	20%
Photopeak Efficiency	45%	73%

Table 1: Assumptions affecting the calculation for estimated transmission and scatter event rates.

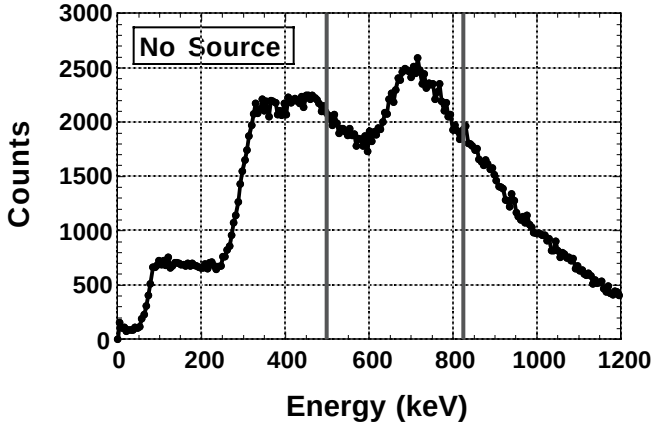

Figure 1: Natural background radiation spectrum of LSO readout with photomultiplier tube. The total natural background activity is measured to be 241 cps/cc, with 99 cps/cc within a 25% energy window centered on the ^{137}Cs photopeak (*i.e.*, 500 – 825 keV). The vertical bars indicate this ^{137}Cs photopeak window.

To estimate the background rate from ^{176}Lu, we measure the self-activated pulse height spectrum from a 10.5 x 10.7 x 13.7 mm^3 piece of LSO attached to a 1" square Hamamatsu 2497 photomultiplier tube. We plot the resulting spectrum in Figure 1. The total background activity measured (*i.e.*, the count rate, independent of deposited energy) is 241 cps/cc, in agreement with previous measurements [1, 21]. Of this background, 99 cps/cc is within a 25% energy window centered on the 662 keV ^{137}Cs photopeak (*i.e.*, 500 - 825 keV).

Results

Figure 2(a) shows the estimated transmission, scatter, and LSO background rates, as a function of transmission source activity, for a single detector module using the "high" performance detector assumptions described in the previous section. Notice that the 7.7 kcps ^{176}Lu background rate dominates the total count rate for lower source strengths. To date, no PET camera has incorporated a singles transmission source with an activity above 20 mCi [20, 22, 23] but this plot states that the background rate exceeds the mean transmission rate for source strengths below 15 mCi and the transmission rate at maximum attenuation for source strengths below 65 mCi. The scattered event rates for both collimated and uncollimated transmission sources are a small fraction of the total event rate at all activities, implying that the affect of transmission source collimation can be neglected when evaluating the affect of ^{176}Lu background. Figure 2(b) shows the same data for a "low" performance detector module, demonstrating similar trends.

Figure 3 shows the transmission NECR as a function of transmission source strength for both the "high" and "low" performance modules. Also shown in this figure are the transmission NECR curves that would be obtained if there were no background

from ^{176}Lu. A significant reduction in the NECR is evident, especially for lower source strengths.

(a)

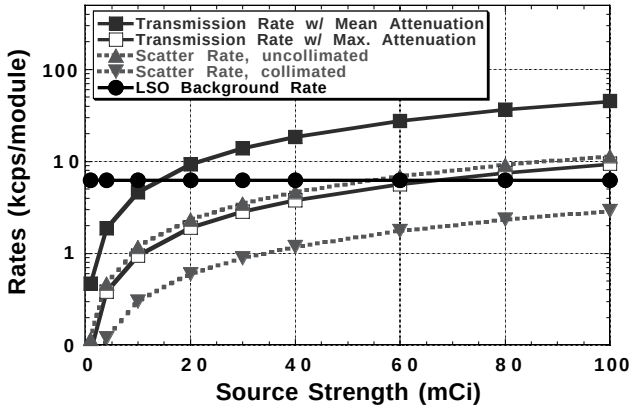

(b)

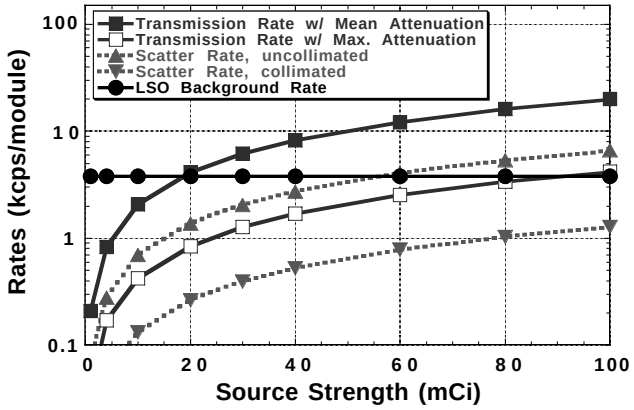

Figure 2: Estimated transmission, scatter, and LSO background rates as a function of source activity for a single detector module with (a) "high" and (b) low performance. The natural background radiation is greater than the mean transmission rate for sources less than 15 mCi (19 mCi) for the "high" ("low") performance detector module.

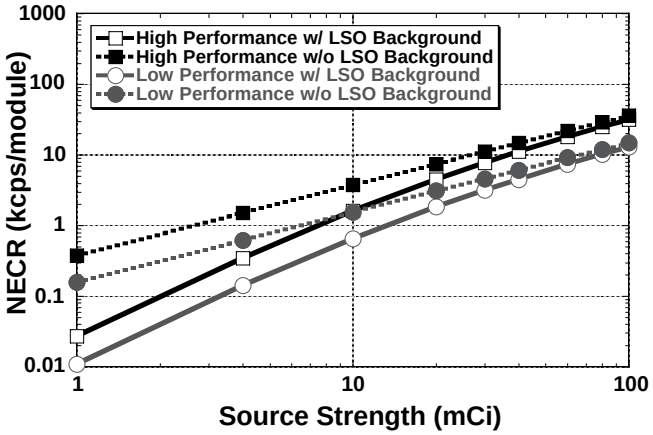

Figure 3: Transmission NECR for mean attenuation as a function of source strength, shown for both "high" (square) and "low" (circle) performance camera detector

modules obtained with (solid) and without (dashed) background from ^{176}Lu. The natural background radiation is seen to have a large effect on the transmission NECR at lower source strengths.

Figure 4 shows the "high" performance module data shown in Figure 3, but re-plotted as the NECR with ^{176}Lu background activity divided by the NECR without the background activity. This quantifies the factor by which the ^{176}Lu background "dilutes" the transmission data, and implies that for mean attenuation and a 10 mCi source, the NECR with background is only 40% of that without background. This dilution factor is identical for the "low" and "high" performance assumptions (within 6% or less for all source strengths), suggesting that the affect of the background is nearly independent of the detector module assumptions. However, similar calculations (also plotted in Figure 4) show that the effect of the background is not significant for the unattenuated ("blank") rate, and that the effect on coincidence data (including randoms) is negligible (not shown).

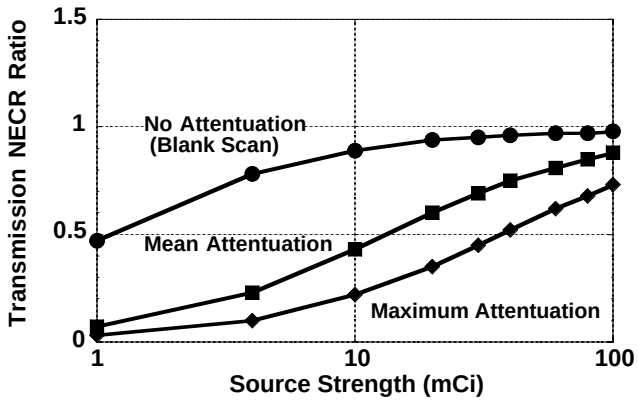

Figure 4: Transmission NECR ratio = Transmission NECR w LSO / Transmission NECR without LSO present, shown for "high" performance camera with a range of attenuation levels. Natural background radiation has a large effect on the NECR particularly for maximum attenuation. The effect of the background is virtually the same for the "low" and "high" performance cameras (with an overall mean difference of less than 1%), so the "low" performance data is not shown.

Discussion and Conclusion

We have shown that the natural background radiation from ^{176}Lu has a significant effect when performing singles transmission. We predict that this background reduces the

mean transmission NECR by a factor of 4.4, 2.3, and 1.4 when using a 4, 10 and 40 mCi source, respectively. These reduction factors are remarkably insensitive to many of the assumptions made. In particular, they are independent of module size, number of transmission sources, and number of modules illuminated by each transmission source. They are virtually independent of a number of module performance factors (scintillator depth, dead time, and photopeak efficiency) and transmission source collimation. They will depend on ring diameter and source orbit diameter, but the general conclusion (that background is a significant factor) remains unchanged.

The NECR for blank scans decreases by only 13%, 6%, and 2% using a 4, 10 and 40 mCi source respectively for both collimated and uncollimated transmission data. Thus, the ^{176}Lu background has little effect on the blank scan but has a large effect on the singles transmission scan. Even with a 20 mCi source, the transmission scan time must increase 67% to maintain the same level of signal-to-noise ratio obtained with a background-free scintillator.

These results suggest that single photon transmission imaging with a whole body LSO-based PET camera requires a stronger source, as well as longer scan times, compared with a standard whole body PET camera. However, there are clearly practical limitations on how large the transmission source strength can be for clinical applications. Different shielding would be required to use ~100 mCi sources because current shielding would not be adequate, and "leakage" from such large transmission sources may affect the emission data. There might also be licensing and safety issues for these higher sources**.** Blank scans would have count rate issues if the camera is not designed to handle ~1 Mcps per detector module.

Acknowledgements

This work was supported in part by the Director, Office of Science, Office of Biological and Environmental Research, Medical Science Division of the U.S. Department

of Energy under Contract No. DE-AC03-76SF00098, and in part by the National Institutes of Health, National Cancer Institute under grant No. RO1-CA67911, and National Institutes of Health, National Heart, Lung and Blood Institute under grant No. P01-HL25840.

1. C. L. Melcher and J. S. Schweitzer, "Cerium-doped lutetium oxyorthosilicate: a fast, efficient new scintillator," *IEEE Trans Nuc Sci*, vol. 39, pp. 502-5, 1992.
2. S. R. Cherry, Y. Shao, R. W. Silverman, et al., "MicroPET: a high resolution PET scanner for imaging small animals," *IEEE Trans Nucl Sci*, vol. 44, pp. 1161-6, 1997.
3. A. F. Chatziioannou, S. R. Cherry, Y. Shao, et al., "Performance evaluation of microPET: A high resolution LSO PET scanner for animal imaging.," *J Nucl Med*, vol. 40, pp. 1164-75, 1999.
4. R. Slates, S. Cherry, A. Boutefnouchet, et al., "Design of a small animal MR compatible PET scanner," *IEEE Trans Nucl Sci*, vol. NS-46, pp. 565-70, 1999.
5. S. Siegel, J. Vaquero, L. Aloj, et al., "Initial results from a PET planar small animal imaging system," *IEEE Trans Nucl Sci*, vol. NS-46, pp. 571-5, 1999.
6. J. A. Correia, C. A. Burnham, D. Kaufman, et al., "Development of a small animal PET imaging device with resolution approaching 1 mm," *IEEE Trans Nucl Sci*, vol. NS-46, pp. 631-5, 1999.
7. A. Saoudi and R. Lecomte, "A novel APD-based detector module for multi-modality PET/SPECT/CT scanners," *IEEE Trans on Nucl Sci*, vol. NS-46, pp. 479-84, 1999.
8. J. S. Huber and W. W. Moses, "Conceptual design of a high sensitivity small animal PET camera with 4π coverage," *IEEE Trans Nucl Sci*, vol. NS-46, pp. 498-502, 1999.
9. M. Schmand, L. Eriksson, M. E. Casey, et al., "Performance results of a new DOI detector block for a high resolution PET-LSO research tomograph HRRT," *IEEE Trans Nucl Sci*, vol. 45, pp. 3000-6, 1998.
10. B. Pichler, C. Boning, E. Lorenz, et al., "Studies with a prototype high resolution PET scanner based on LSO-APD modules," *IEEE Trans Nucl Sci*, vol. 45, pp. 1298-302, 1998.
11. O. Fries and S. M. Bradbury, "A small animal PET prototype based on LSO crystals read out by avalanche photodiodes.," *Nucl. Instrum. and Meth. A*, vol. 387, pp. 220-4, 1997.
12. W. W. Moses, P. R. G. Virador, S. E. Derenzo, et al., "Design of a high-resolution, high-sensitivity PET camera for human brains and small animals," *IEEE Trans. Nucl. Sci.*, vol. NS-44, pp. 1487-91, 1997.
13. R. A. deKemp and C. Nahmias, "Attenuation correction in PET using single photon transmission measurement," *Medical Physic*, vol. 21, pp. 771-8, 1994.
14. S. K. Yu and C. Nahmias, "Single-photon transmission measurements in positron tomography using Cs-137," *Phys. Med. Biol.*, vol. 40, pp. 1255-66, 1995.

15. J. S. Karp, G. Muehllehner, H. Qu, et al., “Singles transmission in volume-imaging PET with a Cs-137 source,” *Phys. Med. Biol.*, vol. 40, pp. 929-44, 1995.

16. D. L. Bailey, “Strategies for accurate attenuation correction with single photon transmission measurements in 3D PET,” *Conference Record of the 1997 Nuclear Science Symposium and the Medical Imaging Conference*, vol. 2, pp. 1009-13, 1997.

17. R. J. Smith, J. S. Karp, F. Benard, et al., “A comparison of segmentation and emission subtraction for singles transmission in PET,” *IEEE Trans Nucl Sci*, vol. 45, pp. 1212-18, 1998.

18. S. C. Strother, M. E. Casey, and E. J. Hoffman, “Measuring PET scanner sensitivity: relating countrates to image signal-to-noise ratios using noise equivalents counts.,” *IEEE Trans Nucl Sci*, vol. 37, pp. 783-8, 1990.

19. C. W. Stearns and D. C. Wack, “A noise equivalent counts approach to transmission imaging and source design,” *IEEE Trans Med Imag*, vol. 12, pp. 287-92, 1993.

20. C. C. Watson, A. Schaefer, W. K. Luk, et al., “Clinical Evaluation of Single-Photon Attenuation Correction for 3D Whole-Body PET,” *IEEE Trans Nucl Sci*, vol. 46, pp. 1024-1031, 1999.

21. T. Ludziejewski, K. Moszynska, M. Moszynski, et al., “Advantages and limitations of LSO scintillator in nuclear physics experiments,” *IEEE Trans Nucl Sci*, vol. 42, pp. 328-36, 1995.

22. J. S. Karp, S. Surti, R. Freifelder, et al., “Performance of a GSO Brain PET Camera,” *Conference Record of the 2000 Nuclear Science Symposium and the Medical Imaging Conference*, 2000.

23. K. Wienhard, M. Schmand, M. E. Casey, et al., “The ECAT HRRT: Performance and First Clinical Application of the New High Resolution Research Tomograph,” *Conference Record of the 2000 Nuclear Science Symposium and the Medical Imaging Conference*, pp. 17/2-6, 2000.